Use of KMAH index in seismic data processing

Georgy Mitrofanov, IGG /SB RAS, Russia
Viatcheslav Priimenko, LENEP/UENF, Brazil

Abstract

We discuss some aspects of the application of KMAH index in seismic data processing. The index can be useful when *a priori* information about a model of medium is available and the corresponding ray tracing can be done. It provides an opportunity to select areas in reflected seismic waves where the ray crosses a caustic. Such areas drastically reduce the quality of seismic sections, as well as worse the separation of signals related to target reflected horizons. Importance of using the KMAH index increases when structure of the model is known and it is required a detail study of the shape of seismic signal. Also, the index may be important in the solution of such tasks as extraction of signals, related to converted waves, for instance, the *PSP*-waves, from surface marine seismic data.

Introduction

The theoretical importance of the KMAH index in the solution of direct geophysical problems and ray tracing is well known (Cerveny at al, 1988; Chapman, 2004). However, in solving practical problems related to real seismic data processing the index is hardly ever used. While the existing ray tracing methods allow determining values of the index for various complex models of media (Cerveny, 2001). Therefore, in the processing of real data such calculations are not difficult to perform if there is *a priori* model for the area under study. Especially the values of KMAH index may be useful in studying media with a complex structure and properties when details of seismic signals form are important.

We present the results on the use of the KMAH index in the separation of reflected signals of both monotype and not monotype waves. Thus there were obtained formulas allowing to calculate its values in the solution of the two-point ray tracing problem.

Method

The KMAH index is one of the important characteristics of geometric seismics (Cerveny, 2001). It is associated with the Jacobean $J(s,r)$ of the transformation of the ray coordinates to Cartesian ones. This relation consists in the following equality:

$$\operatorname{sign}(J(s,r)) = \begin{cases} +1, & \text{if the index is even,} \\ -1, & \text{if the index is odd.} \end{cases} \qquad (1)$$

Here s and r are the start and end points of the ray $R(s,r)$. Usually s and r coincide with the points of the source and receiver. The KMAH index allows to define the number of caustics and focusing situations (focusing can be seen as a double caustic). Thus, determining the values of $J(s,r)$, we can find the values of KMAH index and set appropriate geometric features of rays.

Jacobian $J(s,r)$ can be calculated as in the ray tracing of a single ray $R(s,r)$ and in solving the corresponding two-point problem. In the latter case, mixed second derivatives, involved in the process of constructing an appropriate solution, are used effectively (Mitrofanov and Priimenko, 2013). In the case of *PP*-wave connection with derivatives is determined by the following formula (Goldin, 1986, p.118):

$$J(s,r) = -\frac{\cos\nu_s \cos\nu_r}{V_p^2(s)} \det\left(\frac{\partial^2 t^{PP}(s,r)}{\partial s\, \partial r}\right)^{-1} \qquad (2)$$

where ν_s and ν_r are respectively angles of departure and arrival of the ray from source and receiver (Fig. 1). The similar form for converted waves can be constructed too.

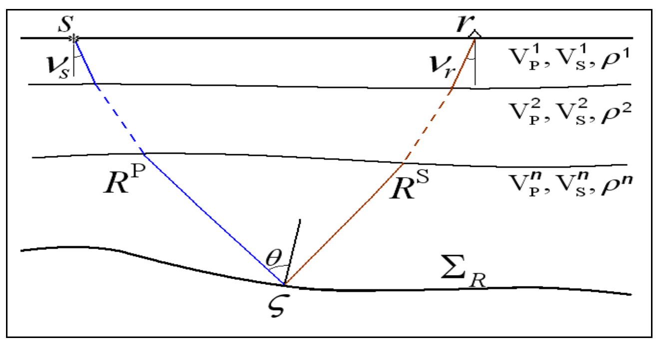

Figure 1. Schematic ray path

Consider the ray corresponding to a fixed *PS*-wave, see Fig. 1. Without loss of generality, assume that the points s and r are located on a horizontal surface of observations. This ray can be split into two parts: $R^P(s,\varsigma)$ and $R^S(\varsigma,r)$, related to the incident *P*-wave, propagating from the source s to the reflection point ς, and the reflected *S*-wave, propagating from ς to the receiver r, respectively. The point ς belongs to a reflective curved boundary Σ_R. In Fig. 1, these parts are shown in blue and brown. Therefore, R^{PS} and R^P, R^S are functions of three parameters (s,r,ς). However, unlike the ray its parts depend on the combination of two parameters: (s,ς) and (r,ς). Thus, we can use the following representation:

$$R^{\mathrm{PS}}(s,r;\varsigma)=R^{\mathrm{P}}(s,\varsigma)+R^{\mathrm{S}}(\varsigma,r). \quad (3)$$

The parameter ς has some special condition in this presentation. It connects with the following. When coordinates of s and r are fixed the coordinate of ς is the variable. Also one more reason concerned these coordinates will be useful for next constructions. Points s and r are independent but the point ς is dependent from them, i.e. $\varsigma=\varsigma(s,r)$. At the same time either of the two points s and r can be dependent on ς, i.e., $s=s(\varsigma)$ и $r=r(\varsigma)$.

Some exclusivity in this representation for the parameter ς related to the fact that when the coordinates s,r are fixed, then the point of reflection can be variable. Also, another consideration regarding these coordinates will be useful: points s and r are independent, but they determine the point ς, i.e., $\varsigma=\varsigma(s,r)$. In addition, each of the two points s and r may be dependent on ς, i.e., $s=s(\varsigma)$ and $r=r(\varsigma)$.

Travel time of the converted wave, propagated from the point s to the point r can be represented by an integral along $R^{\mathrm{PS}}(s,r)$, or as a sum of integrals over each part of the ray. Then, according to Eq. (3), it is a function of the same parameters, i.e.

$$t^{\mathrm{PS}}(s,r;\varsigma)=t^{\mathrm{P}}(s;\varsigma)+t^{\mathrm{S}}(r;\varsigma) \quad (4)$$

Here we do not indicate the dependence of travel time on a priori parameters of the model, as they will be considered in the process of integration. Now, differentiating Eq. (4) by s and after that by r, and taking into account $r=r(\varsigma)$, we obtain

$$\frac{\partial t^{\mathrm{PS}}}{\partial s}=\frac{\partial t^{\mathrm{P}}}{\partial s};$$

$$\frac{\partial}{\partial r}\left(\frac{\partial t^{\mathrm{PS}}}{\partial s}\right)=\frac{\partial}{\partial r}\left(\frac{\partial t^{\mathrm{P}}}{\partial s}\right)=\frac{\partial^2 t^{\mathrm{P}}}{\partial s\partial\varsigma}\cdot\frac{\partial\varsigma}{\partial r};$$

$$\frac{\partial}{\partial r}\left(\frac{\partial t^{\mathrm{PS}}}{\partial s}\right)=\frac{\partial^2 t^{\mathrm{PS}}}{\partial s\partial r}+\frac{\partial t^{\mathrm{PS}}}{\partial\varsigma}\cdot\frac{\partial\varsigma}{\partial r}.$$

But the point of reflection ς of this ray is found according to the principle of Fermat. Therefore, the first derivative of (4) is zero. Consequently

$$\frac{\partial^2 t^{\mathrm{PS}}}{\partial s\partial r}=\frac{\partial^2 t^{\mathrm{P}}}{\partial s\partial\varsigma}\cdot\frac{\partial\varsigma}{\partial r}.$$

Now we need to find $\partial\varsigma/\partial r$. To this effect consider

$$\frac{\partial}{\partial r}\left(\frac{\partial t^{\mathrm{PS}}}{\partial\varsigma}\right)=\frac{\partial^2 t^{\mathrm{S}}}{\partial\varsigma\partial r}+\left(\frac{\partial^2 t^{\mathrm{P}}}{\partial\varsigma}+\frac{\partial^2 t^{\mathrm{S}}}{\partial\varsigma}\right)\cdot\frac{\partial\varsigma}{\partial r}.$$

It is also equal to zero, according to the principle of Fermat. Hence

$$\frac{\partial\varsigma}{\partial r}=-\left(\frac{\partial^2 t^{\mathrm{P}}}{\partial\varsigma^2}+\frac{\partial^2 t^{\mathrm{S}}}{\partial\varsigma^2}\right)^{-1}\cdot\frac{\partial^2 t^{\mathrm{S}}}{\partial\varsigma\partial r}.$$

Thus, the final expression is

$$\frac{\partial^2 t^{\mathrm{PS}}}{\partial s\partial r}=-\frac{\partial^2 t^{\mathrm{P}}}{\partial s\partial\varsigma}\cdot\left(\frac{\partial^2 t^{\mathrm{P}}}{\partial\varsigma^2}+\frac{\partial^2 t^{\mathrm{S}}}{\partial\varsigma^2}\right)^{-1}\cdot\frac{\partial^2 t^{\mathrm{S}}}{\partial\varsigma\partial r}. \quad (5)$$

Substituting in Eq. (2) the second derivative of the *PP*-wave by Eq. (5) for the *PS*-wave, we arrive at

$$J(s,r)=\frac{\cos\nu_s\cos\nu_r}{\mathrm{V}_{\mathrm{p}}^2(s)}\cdot$$

$$\cdot\det\left[\left(\frac{\partial^2 t^{\mathrm{P}}}{\partial s\partial\varsigma}\right)^{-1}\cdot\left(\frac{\partial^2 t^{\mathrm{P}}}{\partial\varsigma^2}+\frac{\partial^2 t^{\mathrm{S}}}{\partial\varsigma^2}\right)\cdot\left(\frac{\partial^2 t^{\mathrm{S}}}{\partial\varsigma\partial r}\right)^{-1}\right]. \quad (6)$$

We see, that unlike Eq. (4), it includes not only the second derivatives with respect to the receiver and source points, but also derivatives with respect to the reflection point ς, where occurs the formation of the converted *PS*-wave.

Eq. (6) can be used both in the determination of the values of KMAH index by Eq. (1) and in determining the amplitude using zero approximation of the ray series

$$A^{\mathrm{PS}}(s,r;\varsigma)=$$

$$=A_0K^{\mathrm{PS}}(\varsigma)\frac{\Pr(s,r)}{\sqrt{|J(s,r)|}}\sqrt{\frac{\mathrm{V}_{\mathrm{p}}^1(s)}{\mathrm{V}_{\mathrm{S}}^1(r)}\cdot\frac{\rho^1(s)}{\rho^1(r)}}, \quad (7)$$

where A_0 - amplitude of the initial signal, $K^{\mathrm{PS}}(\varsigma)$ - reflection coefficient of the *PS*-wave, $J(s,r)$ - square geometrical spreading, $\Pr(s,r)$ is a function, which includes all other factors considered in the zero approximation (characteristics of the source and receiver orientation, product of the refraction coefficients, conversion rate, etc.), $\mathrm{V}_{\mathrm{P}}^1(s)$ and $\mathrm{V}_{\mathrm{S}}^1(r)$ are the velocity of propagation of corresponding waves in a vicinity of the source s and receiver r, $\rho^1(s)$ and $\rho^1(r)$ are the corresponding densities.

Results

The calculation procedures and criteria of utilization of the KMAH index in the surface seismic data processing are based on Eqs. (1)-(2), (6) and (7). They allow us to analyze the possible occurrence of caustic situations for converted and non-converted waves. This provides a basis for selecting the respective areas and removing many-valuedness in the separation of target signals. The use of procedures in the processing of synthetic data corresponding to real reservoirs (Mitrofanov and Priimenko, 2013) indicated the following.

1. Considerable caustic areas can be reliably identified, as on the basis of the visual analysis of seismograms and in automatic mode, based on the values of KMAH index. However, in the case of small caustic domains when their position changes significantly for different source and receiver arrays, such identification is possible only using the values of this index.
2. Regardless of the size of caustic domain, it results in significant changes in the structure of hodographs of the reflected waves. Taking place "break" of the hodograph may lead to a significant deviation of its structure from the approximation hyperbole and, especially, from the parabola. Such deviations can reach tens of milliseconds; it does not allow the selection of the reflected signals by directed summation.
3. Joint utilization of the KMAH index and amplitudes permits to determine optimal observation areas of for the selection of the target signal with the highest signal-to-noise ratio. It can play an important role in detecting the weak signals of non-converted waves and signals of converted waves such as, for example, *PSP*-waves.

Examples

We shall discuss several examples related to model experiments performed for an offshore oil field. The structure of the models and a general view of synthetic seismograms are presented in the paper (Mitrofanov and Priimenko, 2013). Therefore, here we demonstrate only using the KMAH index as well the amplitudes for the selection of observations and preparation of data to the $\tau - p$ transformation.

Consider one of the synthetic seismograms, constructed by the ray tracing method (Fig. 2), where an identification of target signals related to the *PP* and *PSP*-waves was done. Under identification we used the calculated values of travel times $t(s,r)$ of the corresponding waves. On the seismogram clearly shows that in the relevant area there are two caustics, corresponding to the *PP* and *PSP* waves reflected from the fifth horizon of the *a priori* model. Subsequently, these events are marked as *PP5* and *PSP5* respectively.

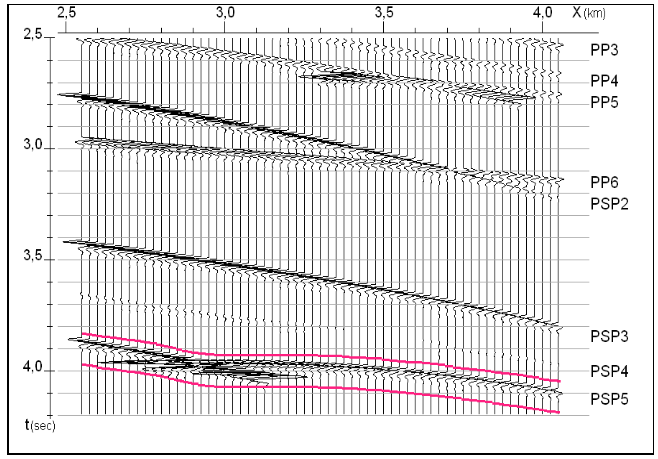

Figure 2. Synthetic seismogram

Manual selection of the interval that contains signals corresponding to the reflected *PSP5*-wave, allows a detailed study of their features. Fig. 3 shows (top to bottom): the selected intervals, the energy, the values of the amplitude and phase spectra calculated for the signals corresponding to these intervals. It is seen that in the caustic domain the reflected signals have significant differences in their shape and properties. The observed caustic domain can be simply recognized on the basis of a detailed analysis of ray schemes and arrival times $t(s,r)$, calculated for the corresponding wave (see Fig. 4).

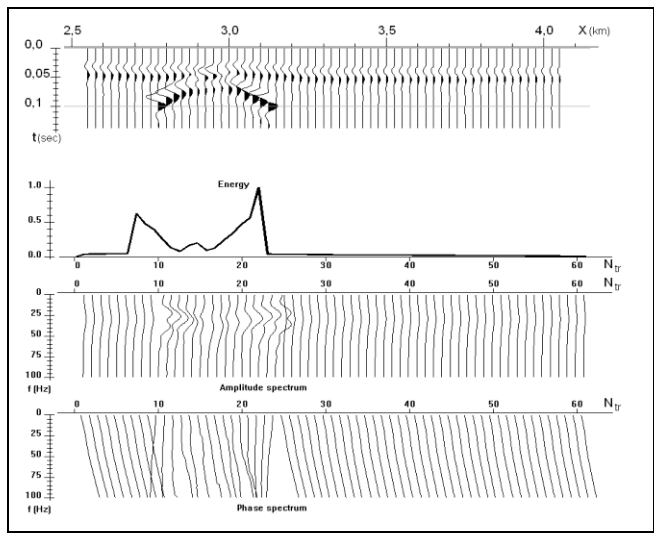

Figure 3. Characteristics of the signals related to caustic domain

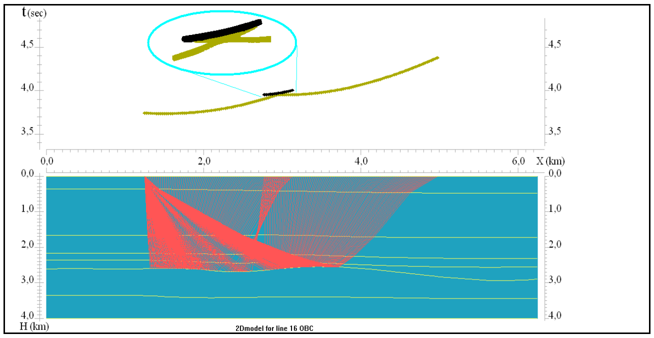

Figure 4. Rays and travel times calculated for *PSP5*-wave

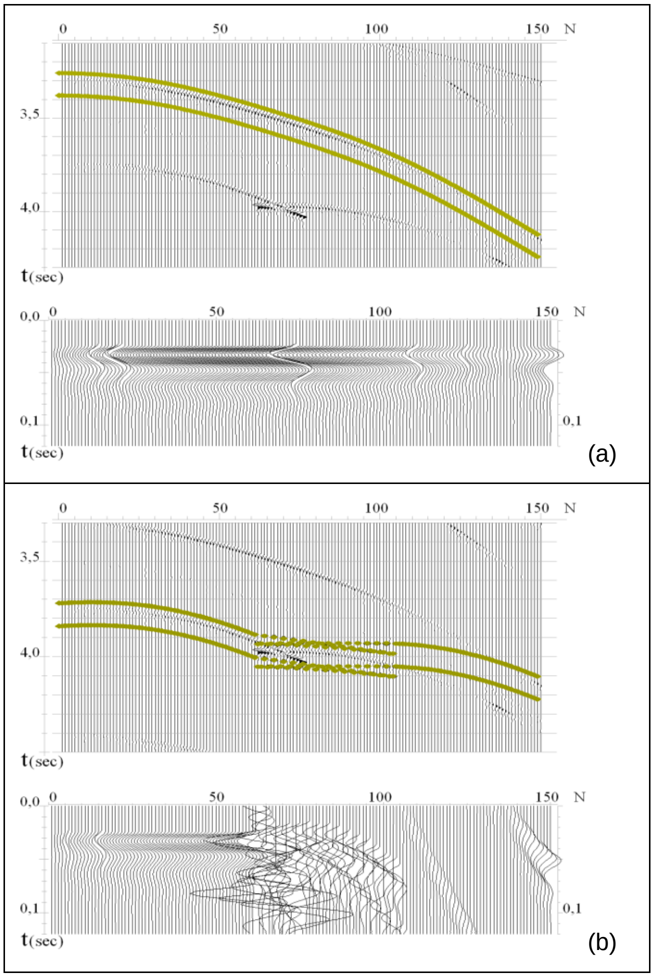

Figure 5. Selection of time intervals for the cases of absence (a) and presence (b) of caustic domains

However, the situation will be more complex in the case of automatic selection of time intervals using only arrival times for the signals of given waves. When caustics are not available, the selection does not cause difficulties. Fig. 5(a) shows the result of such automatic selection for the *PSP3*-wave. This wave has not any caustic singularity in this area. Fig. 5(b) presents a different result, where the *PSP5*-wave was automatically selected. In this case the caustic singularities lead to significant errors. This is connected with the ambiguity in the definition of lines for the selection of intervals.

The essential point in the determination of caustic region is its size. In the case of extended enough domain such area is easier to identify. The identification turns much difficult in the case of small domain. Figs. 6 and 7 show (in black color) the position of caustic regions in multiple observations. They are related to the reflected *PP* and *PSP*-waves, which correspond to the two types of models that have large and small caustic regions.

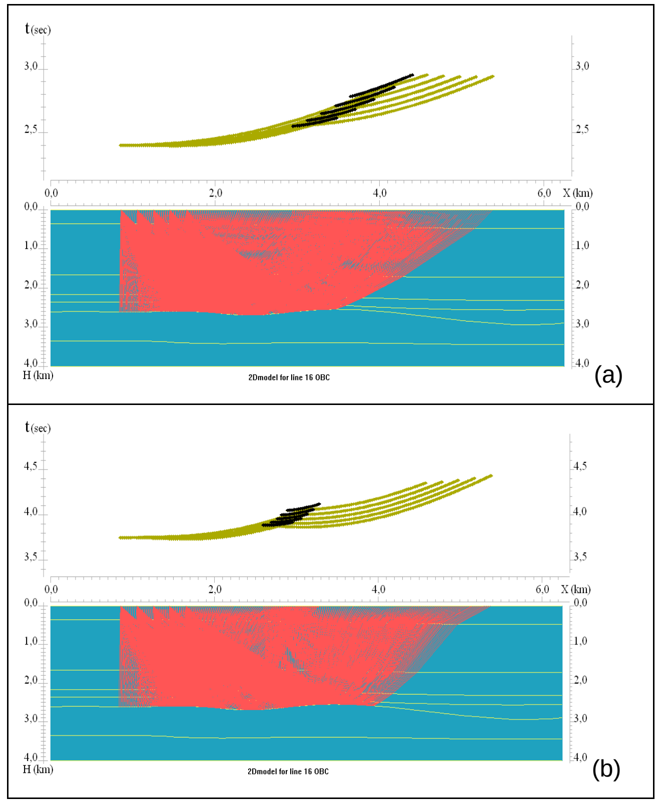

Figure 6. Extended caustic areas for *PP* (a) and *PSP* (b) waves

But independently of width of region the caustic will exert considerable influence on the intervals selection and results of coherent summing of signals. Therefore, we need to identify the corresponding areas in the wave field and system observations. For this purpose the values of KMAH index can be useful.

In Fig. 8 the values of KMAH index, which are corresponded to two different kinds of caustic domain, are presented. As shown in the picture for both cases these values give possibilities to identify the caustic region exactly. Note that the small caustic region demonstrated at Fig. 7 had been found out just by such values.

After determination of caustic regions the correct selection of time intervals can be provided without difficulties. Some examples of such selection are shown in Fig. 9.

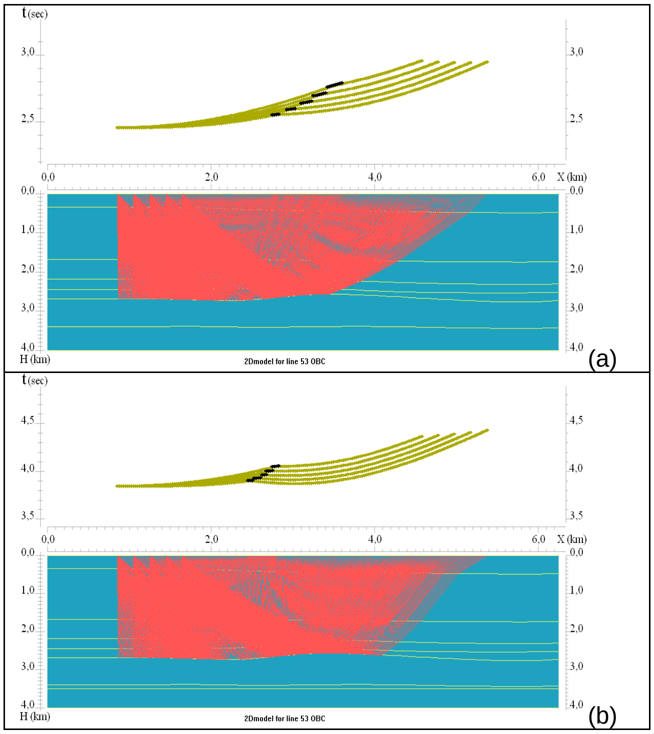

Figure 7. Small caustic areas for *PP* (a) and *PSP* (b) waves

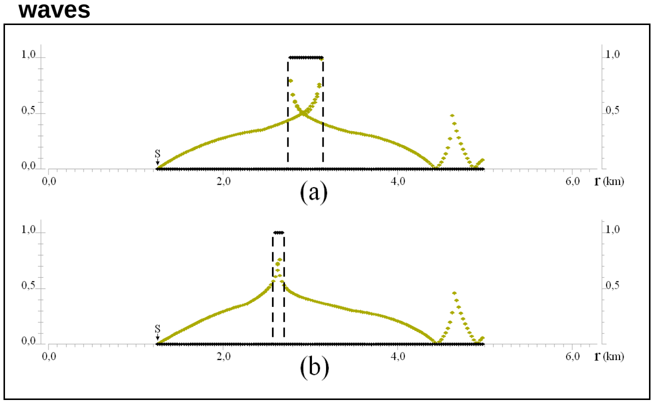

Figure 8. Values of KMAH index (black color) and amplitude $A^{PS}(s,r;\varsigma)$ (brown color) calculated for the extended (a) and small (b) caustic domains

Conclusions

Using these results, we have demonstrated the importance of using the KMAN-index to determine caustic features that can be observed in the case of complex models. It provides the correct selection of time intervals in the analysis and processing of the target signals, which may improve the accuracy of the corresponding tasks.

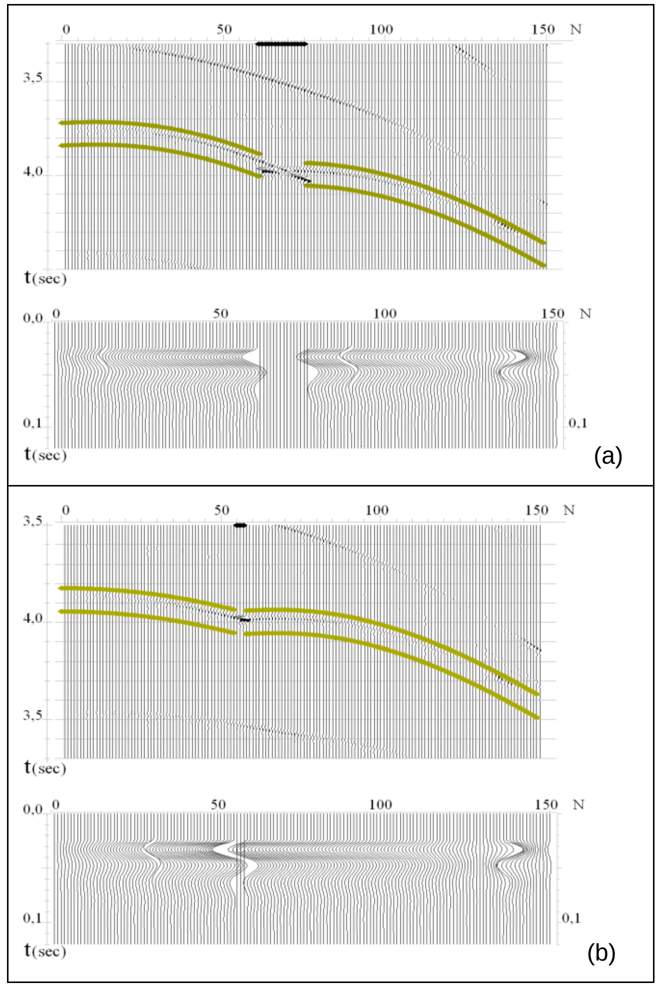

Figure 9. Time intervals selected using the KMAH index for the cases of extended (a) and small (b) caustic domains

References

1. **Cerveny V., Klimes L. & Psencik I. 1988.** Complete seismic-ray tracing in three-dimensional structures. In: Seismological Algorithms, pp.89-168, ed. Doornbos D.J., Academic Press, New York.
2. **Cerveny V. 2001.** Seismic Ray Theory, Cambridge Univ. Press.
3. **Chapman C. 2004.** Fundamentals of Seismic Wave Propagation. Cambridge Univ. Press.
4. **Goldin S.V. 1986.** Seismic Traveltime Inversion. Investigations in Geophysics, Society of Exploration Geophysics.
5. **Mitrofanov G. & Priimenko V. 2013.** Separation of *PSP*-waves on marine seismic data. In: 13th International Congress of the Brazilian Geophysical Society & EXPOGEF, 2013, Rio de Janeiro.

Acknowledgments

This work was supported by the Petrobras Institute for Research and Development - CENPES, RJ, Brazil.